Dynamics of bulk fluctuations in a lamellar phase studied by coherent X-ray scattering

Doru Constantin,[1,*] Guillaume Brotons,[2] Tim Salditt,[3] Éric Freyssingeas,[1] and Anders Madsen[4]

[1] *École Normale Supérieure de Lyon, Laboratoire de Physique, 46 Allée d'Italie, 69364 Lyon Cedex 07, France*
[2] *Laboratoire de Physique de l'État Condensé, Université du Maine, Faculté des Sciences et techniques, Av. O. Messiaen – 72085 Le Mans Cedex 9, France*
[3] *Institut für Röntgenphysik, Georg-August-Universität Göttingen, Friedrich-Hund-Platz 1, D-37077 Göttingen, Germany*
[4] *European Synchrotron Radiation Facility, Boîte Postale 220, 38043 Grenoble, France*

(Dated: April 9, 2015)

Using X-ray photon correlation spectroscopy, we studied the layer fluctuations in the lamellar phase of an ionic lyotropic system. We measured the relaxation rate of in-plane (undulation) fluctuations as a function of the wave vector. Static and dynamic results obtained during the same experiment were combined to yield the values of both elastic constants of the lamellar phase (compression and bending moduli) as well as that of the sliding viscosity. The results are in very good agreement with dynamic light scattering data, validating the use of the technique in ordered phases.

PACS numbers: 61.30.St, 87.15.Ya, 61.10.-i

I. INTRODUCTION

X-ray Photon Correlation Spectroscopy (XPCS) is a relatively new technique [1], successfully used to study the dynamics of soft-matter systems, such as colloidal dispersions [2, 3], fluid interfaces [4, 5] and free-standing smectic films [6–8]. Although conceptually very similar to the traditional Dynamic Light Scattering (DLS) technique, its main advantages with respect to DLS are the potential of reaching much higher scattering wavevectors and the fact that it is much less affected by multiple scattering.

Among the cited systems, smectic phases are especially adapted to the use of XPCS techniques, since their high degree of order confines the scattered signal in the vicinity of the (quasi) Bragg peaks. To date, these studies were limited to thermotropic smectics at interfaces: either in thin films [9], or at the interface with air [10]; in both cases, the dynamics is driven by the ratio between surface tension and viscosity.

In the present work we use XPCS to measure the dispersion relation of fluctuations in bulk samples of a lamellar lyotropic phase (exhibiting smectic symmetry) and compare the results with DLS measurements. This investigation was mainly prompted by three questions, which we were able to answer in the affirmative:

a. Is the technique applicable to these systems? To our knowledge, XPCS was never applied to lamellar lyotropic phases; although the symmetry is the same as for thermotropic smectics, there are notable differences due to the two-component character of the lyotropic phase (leading to additional hydrodynamic modes), to its lower elastic moduli, which influence both the relaxation rates and the 'spread' of the diffuse scattering around the Bragg position (thus limiting the accessible wave vector range). Finally, the difference in viscosity and electronic contrast can also have an effect.

b. Can we determine the intrinsic elastic moduli of the phase by using bulk samples? In the smectic systems studied so far, the relaxation was driven by the surface tension. The sample thickness at which boundary effects become dominant in the relaxation dynamics depends on the elastic properties of the phase (more specifically, on the penetration length). It should be noted that the compression modulus of lyotropic phases is typically more than three orders of magnitude below that of thermotropic phases. Moreover, the bending modulus can be tuned within certain limits and –in some specific mixtures– the lamellar spacing can be easily varied by more than a factor of ten. Thus, lyotropic smectics provide a much more flexible model system than their thermotropic counterparts.

c. Are the results comparable with those obtained by dynamic light scattering in terms of accessible range, accuracy etc.? This is a crucial question, since the main interest of XPCS is the possibility of complementing and extending the range of DLS experiments. Such a comparison was already performed for colloid suspensions [11, 12], but not in ordered phases. Such a comparison is non-trivial for smectic systems, first of all because XPCS is performed around a Bragg position, while in DLS one probes the vicinity of the origin of reciprocal space.

II. MATERIALS AND METHODS

The SDS/pentanol/H_2O system was extensively used as a model lamellar phase [13–15]. In this work, instead of pure water we use as solvent a 40/60 (wt%) solution of glycerol/H_2O, in order to increase its viscosity and correspondingly reduce the relaxation rates of the fluctuations: $\eta_{\rm sol} = 3.65\,\eta_{\rm H_2O}$ [16]. The sample composition

*Electronic address: constantin@lps.u-psud.fr; Permanent address: Laboratoire de Physique des Solides, Université Paris-Sud, Bât. 510, 91405 Orsay Cedex, France.

by volume is: 19.3 % SDS, 29.9 % pentanol and 50.8 % glycerol/H_2O. The samples were prepared in 100 and 200 μm thick borosilicate glass capillaries (VitroCom Inc.) and oriented by thermal cycling between the lamellar and the isotropic phases, resulting in very good homeotropic anchoring. All measurements were performed at 21.5 °C.

The experiments were performed at the ID10A undulator beamline at ESRF (Grenoble, France) using an X-ray energy of 13 keV selected by a Si (111) single-bounce monochromator, in the uniform filling mode of the storage ring. The beam was defined by a 10μm pinhole followed by a guard slit for removal of parasitic scattering. The scattered signal was detected by a fast avalanche photodiode (APD) and the output signal was processed online by a FLEX autocorrelator.

III. RESULTS AND ANALYSIS

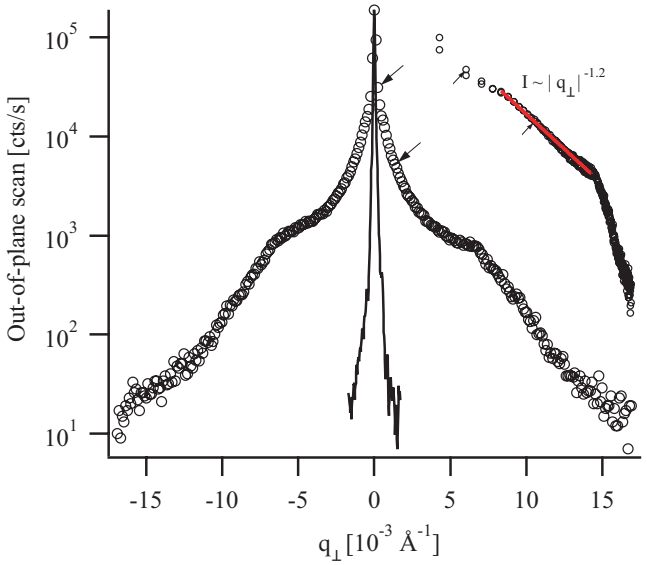

FIG. 1: (Color online) Out-of-plane scan of the first Bragg peak (open symbols) shown in log-lin and log-log (inset) representation. The scan of the primary beam is presented for comparison (solid line) normalized by a factor 10^{-4}. In both graphs, the arrows indicate the range of the XPCS measurements. In the log-log graph, the straight line is the power-law fit to the intensity (see text).

A. Static scattering

The smectic periodicity is $d = 38.7$ Å, somewhat smaller than predicted by the dilution law with pure water, namely 41 Å [15]. It is not clear if this is due to the presence of glycerol and how this component influences the phase diagram of the mixture and the lamellar spacing.

We measured the line shape of the first Bragg peak along the transverse direction, i.e. in the plane of the layers: $I(q_\perp)$ (Figure 1). More precisely, if we take direction z along the normal to the layers and denote by x the projection of the incident beam onto the layers (so that the incidence plane is (xz)), the experimental points correspond to taking the detector out of the plane of incidence, along the y direction: $q_\perp = q_y$.

It is well known that bulk lamellar phases exhibit the Landau-Peierls instability, leading to a characteristic power-law variation of the scattered signal close to the Bragg peak [17] given by $I \sim q_\perp^{-(4-2\eta_c)}$, with the conventional Caillé exponent

$$\eta_c = \frac{\pi}{2d^2}\frac{k_B T}{\sqrt{B\kappa/d}} \tag{1}$$

where B is the compression modulus of the lamellar phase [28] and κ is the bending stiffness of the bilayer.

We observe a clear power-law behaviour out to about $q_\perp = 5\,10^{-3}$Å^{-1}, with an exponent of -1.2, yielding $\eta_c = 1.4$. This "coupled elasticity" regime is followed by a much steeper decay at higher values, corresponding to length scales over which the bilayers fluctuate independently; we measure an exponent of -3.9, very close to the theoretical value of -4.

B. Dynamic scattering (XPCS)

We recorded the time correlation of the diffuse scattered signal in the vicinity of the first Bragg peak, in the same configuration as for the static measurements, over a $q_\perp$ range indicated by the arrows in Figure 1. When close enough to the peak, one can separate the scattering vector into two components:

$$\mathbf{q} = \mathbf{q}_{\rm Bragg} + \mathbf{q}_{\rm def} \tag{2}$$

with $|\mathbf{q}_{\rm def}| \ll |\mathbf{q}_{\rm Bragg}|$, where the Bragg component shows that the lamellar stack is "sampled" with a periodicity corresponding to the lamellar spacing, and the $\mathbf{q}_{\rm def} = \mathbf{q}_\perp + q_z\hat{\mathbf{z}}$ component indicates large-scale superimposed deformations. In general, for a given deformation vector two hydrodynamic modes are coupled with the lamellar order: the second sound [18] (which relaxes much too fast to be detected by our setup) and the baroclinic mode, whereby the system fluctuates at a fixed chemical potential [14, 19]. This is the only mode we shall discuss in the following. As $\mathbf{q}_{\rm def}$ becomes perpendicular to the z-axis ($\mathbf{q}_{\rm def} = \mathbf{q}_\perp$), the undulation limit of the baroclinic mode is reached.

The correlation function $g(t)$ was obtained at each $q_\perp$ value by acquiring the signal for 1800 or 3600 s. After normalization by the autocorrelation of the monitor signal and removal of an oscillatory component due to the mechanical noise of the setup, $g(t)$ was fitted with the sum of a stretched exponential (stretching exponent

$\beta \sim 0.5$) representing the relaxation of the undulation mode and a very slow exponential (decay time $\tau \sim 10$s) of unknown origin:

$$g(t) = 1 + \left[a_1 \exp\left[-(\Omega t)^\beta\right] + a_2 \exp(-t/\tau) + a_3\right]^2 \quad (3)$$

Figure 2 shows the correlation function $g(t)$ determined for an intermediate value of $q_\perp$. Both the raw signal and the smoothed curve were fitted to the same model; they yield the same relaxation rate, but the error bars are smaller; in the following, we only use the smoothed curves.

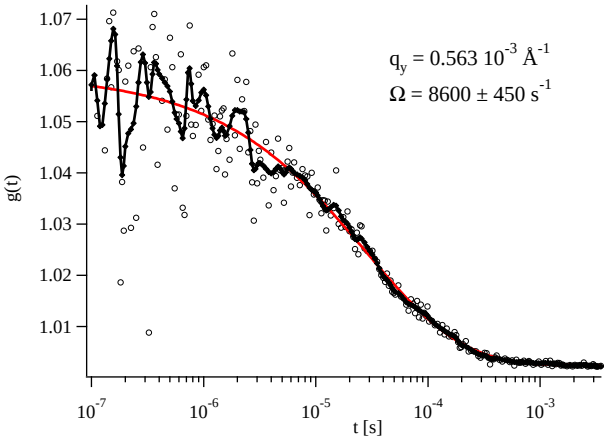

FIG. 2: (Color online) Correlation function $g(t)$ measured for ($q_\perp = 0.563\,10^{-3}$Å^{-1}). Open symbols: raw signal; dots and solid line: smoothed signal; solid line: fit with the model described in the text (equation 3).

The dispersion relation $\Omega(\mathbf{q})$ for fluctuations in the lamellar phase is well known [14, 20, 21]. In the limit of the undulation mode, $q_z = 0$, it reduces to $\Omega(q_\perp) = \frac{\kappa/d}{\eta_3} q_\perp^2$, with κ the bending stiffness, d the lattice spacing and η_3 the layer sliding viscosity [22]. However, this limit cannot be reached since the finite size of the capillary (thickness $D = 100\,\mu$m) imposes a finite $q_z = \pi/D$ component [23] that must be taken into account when describing the dispersion relation, which becomes:

$$\Omega(q_\perp) = \frac{\kappa/d}{\eta_3} q_\perp^2 \left[1 + \left(\frac{\pi}{\lambda D}\right)^2 q_\perp^{-4}\right] \quad (4)$$

where $\lambda = \sqrt{\kappa/(dB)}$ is the penetration length of the smectic phase.

The fit quality is very good, yielding parameters $\kappa/(d\eta_3) = (1.66 \pm 0.06)\,10^{-10}\,\mathrm{m}^2/\mathrm{s}$ and $\lambda = (19.6 \pm 0.4)$ Å. Using the value of $\eta_c = 1.4$ from the power-law dependence of the static scattering, we can determine the elastic moduli and the sliding viscosity as:

$$\begin{aligned} \kappa &= 2.35\,10^{-21}\,\mathrm{J} \simeq 0.58\,k_BT \\ B &= 1.56\,10^5\,\mathrm{Pa} \\ \eta_3 &= 3.65\,10^{-3}\,\mathrm{Pa\ s} \end{aligned} \quad (5)$$

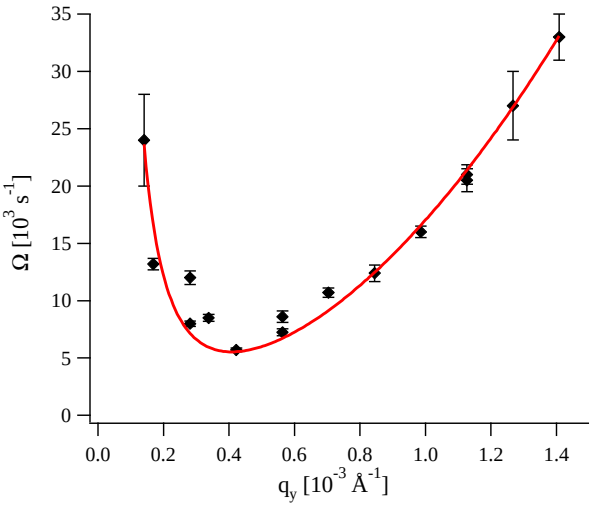

FIG. 3: (Color online) Measured relaxation rates (diamonds) and fit with the dispersion relation (Eq. 4) shown as solid line.

First of all, we note that the value found for the sliding viscosity is exactly that of the solvent: $\eta_3 \simeq \eta_{\mathrm{sol}}$, as expected. The bending modulus κ is similar to that measured from the dilution law $d(\phi)$ [15], which decreases abruptly with the increasing water thickness d_w and saturates at about $0.3\,k_BT$ for $d_w > 20$ Å. In our system, $d_w \simeq 18.5$ Å, and a more precise comparison is difficult to make. In the following section we further check our results against those of light scattering experiments.

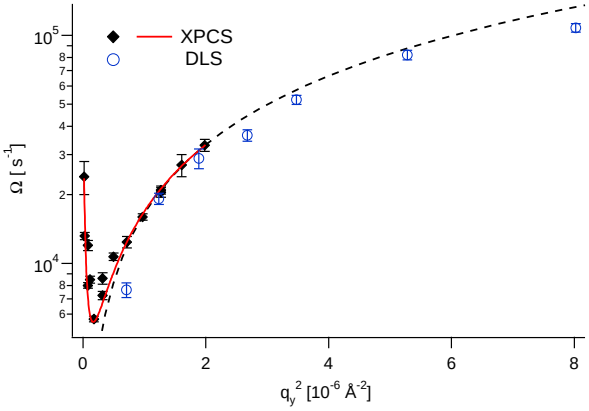

FIG. 4: (Color online) Comparison between the XPCS and DLS results. Diamonds and solid line: XPCS data and fit (as in Fig. 3). Dotted line: high-$q_\perp$ extrapolation of the fit. Open dots: DLS results.

C. Light scattering (DLS)

The experimental DLS setup is described in reference [24]. Briefly, it uses the green (514 nm) emission line of an

Ar laser (Coherent Innova 305) and the scattered signal is collected with a photon-counting PMT. We only investigated the undulation mode, corresponding to a scattering vector $q_\perp$ contained within the plane of the layers.

The relaxation rate of the undulation mode was measured in DLS for $q_\perp$ between 0.84 and $2.3\,10^{-3}\text{Å}^{-1}$; the experimental points are shown as open dots in Figure 4. They agree very well with the measured XPCS points (solid diamonds) and the extrapolated dispersion relation for the undulation mode (dotted line), although they are systematically lower. It is noteworthy that the correlation functions measured in DLS exhibit the same stretching exponent $\beta \sim 0.5$ as the XPCS ones; thus, the stretching is not resolution-induced.

IV. CONCLUSION

We demonstrated the use of the XPCS technique for measuring the dispersion relation of the undulation mode in a lyotropic lamellar phase up to a wave vector $q_{\max} = 1.4\,10^{-3}\text{Å}^{-1}$; the results are in very good agreement with dynamic light scattering measurements. Combining XPCS and static diffuse scattering measured on the same sample using the same setup we obtain precise results for the material parameters of the lamellar phase (Eq. 5).

In this work, the accessible q-range is about half that of dynamic light scattering. However, in the case of more contrasted systems with slower dynamics, the DLS range can probably be exceeded. On the other hand, DLS measurements are also difficult at *low* q values, due to impurities and other defects which cannot be easily eliminated in ordered systems. The advantage of XPCS is its selectivity, due to the Bragg "sampling" expressed by Eq. 2, which renders it insensitive to such defects. Thus, it can also be applied to slightly misaligned or "dirty" samples.

A systematic comparison between XPCS (measurements around the Bragg peak) and DLS (probing the origin of reciprocal space) will probably require a more detailed theoretical description than our intuitive explanation, especially as the deformation wave vector $\mathbf{q}_{\text{def}}$ approaches the Bragg value.

The XPCS technique should be particularly interesting for the study of recently discovered systems, such as DNA-lipid complexes [25], where the dynamics of the confined DNA strands could provide further insight into the structure of the 2D 'sliding' phase [26] they form within the host lamellar matrix, or of inorganic lamellar phases [27], where the presence of heavier elements increases the X-ray contrast at the same time it hinders light scattering measurements.

Acknowledgments

DC received financial support from the CNRS through an "Associated researcher" fellowship. We acknowledge fruitful discussions with Jérôme Crassous and Frédéric Nallet.

[1] G. Grübel and F. Zontone, J. Alloys Comp. **362**, 3 (2004).
[2] J. Lal, D. Abernathy, L. Auvray, O. Diat, and G. Grübel, Eur. Phys. J. E **4**, 263 (2001).
[3] A. Robert, J. Wagner, T. Autenrieth, W. Härtl, and G. Grübel, J. Chem. Phys. **122**, 084701 (2005).
[4] H. Kim, A. Rühm, L. B. Lurio, J. K. Basu, J. Lal, D. Lumma, S. G. J. Mochrie, and S. K. Sinha, Phys. Rev. Lett. **90**, 068302 (2003).
[5] A. Madsen, T. Seydel, M. Sprung, C. Gutt, M. Tolan, and G. Grübel, Phys. Rev. Lett. **92**, 096104 (2004).
[6] A. C. Price, L. B. Sorensen, S. D. Kevan, J. Toner, A. Poniewierski, and R. Hołyst, Phys. Rev. Lett. **82**, 755 (1999).
[7] I. Sikharulidze, I. P. Dolbnya, A. Fera, A. Madsen, B. I. Ostrovskii, and W. H. de Jeu, Phys. Rev. Lett. **88**, 115503 (2002).
[8] I. Sikharulidze, B. Farago, I. P. Dolbnya, A. Madsen, and W. H. de Jeu, Phys. Rev. Lett. **91**, 165504 (2003).
[9] I. Sikharulidze and W. H. de Jeu, Phys. Rev. E **72**, 011704 (2005).
[10] A. Madsen, J. Als-Nielsen, and G. Grübel, Phys. Rev. Lett. **90**, 085701 (2003).
[11] D. O. Riese, W. L. Vos, G. H. Wegdam, F. J. Poelwijk, D. L. Abernathy, and G. Grübel, Phys. Rev. E **61**, 1676 (2000).
[12] G. Grübel, D. L. Abernathy, D. O. Riese, W. L. Vos, and G. H. Wegdam, J. Appl. Cryst. **33**, 424 (2000).
[13] C. Safinya, D. Roux, G. Smith, S. Sinha, P. Dimon, N. Clark, and A. Bellocq, Phys. Rev. Lett. **57**, 2718 (1986).
[14] F. Nallet, D. Roux, and J. Prost, J. Phys. (France) **50**, 3147 (1989).
[15] E. Freyssingeas, D. Roux, and F. Nallet, J. Phys. Condens. Matter **8**, 2801 (1996).
[16] D. R. Linde, ed., *Handbook of Chemistry and Physics* (CRC Press, Boca Raton, 1999).
[17] A. Caillé, C. R. Acad. Sci. Paris, Sér. B **274**, 891 (1972).
[18] P.-G. de Gennes and J. Prost, *The Physics of Liquid Crystals* (Oxford University Press, Oxford, 1993).
[19] F. Brochard and P.-G. de Gennes, Pramana Suppl. **1**, 1 (1975).
[20] G. Sigaud, C. W. Garland, H. T. Nguyen, D. Roux, and S. T. Milner, J. Phys. II (France) **3**, 1343 (1993).
[21] P. Štěpánek, F. Nallet, and K. Almdal, Macromolecules **34**, 1090 (2001).
[22] P. C. Martin, O. Parodi, and P. S. Pershan, Phys. Rev. A **6**, 2401 (1972).
[23] R. Ribotta, D. Salin, and G. Durand, Phys. Rev. Lett. **32**, 6 (1974).
[24] E. Freyssingeas, A. Martin, and D. Roux, Eur. Phys. J. E **18**, 219 (2005).

[25] J. O. Rädler, I. Koltover, T. Salditt, and C. R. Safinya, Science **275**, 810 (1997).
[26] T. Salditt, I. Koltover, J. O. Rädler, and C. R. Safinya, Phys. Rev. Lett. **79**, 2582 (1997).
[27] J. C. P. Gabriel, F. Camerel, B. J. Lemaire, H. Desvaux, P. Davidson, and P. Batail, Nature **413**, 504 (2001).
[28] B stands for the compression modulus at fixed chemical potential, often denoted by $\overline{B}$ in the literature.